Finite Element Analysis of Open-type Dielectric / Optical Waveguides

Marcos KOSHIMOTO*, Zaheed MAHMOOD* and Yukio KAGAWA*

(Received October 2 , 1995)

Optical fibers or integrated optical waveguides have arbitrary cross-sectional index or refraction distribution. An efficient finite element method for analyzing the propagation characteristics of dielectric / optical waveguides with open boundary is presented. The propagation modes are hybrid, for which a variational expression is formulated in terms of the longitudinal electric and magnetic field components. Infinite elements are introduced to consider open boundary or to extend the region to infinity. Several specific examples are given and the results are compared with those obtained by other approximate methods. Very close agreements have been found.

1. INTRODUCTION

Optical fibers have been widely used as one of the major transmission media for long distance telecommunication, with very low loss and broad bandwidth. In the design of their structure, it is important to calculate the propagation characteristics of the guided modes, and to do that, several numerical analysis methods have been proposed. Among them, the finite element method has emerged as one of the most generally applicable and versatile methods for the analysis of waveguides. With FEM, the waveguide is treated as an eigenvalue problem with inhomogeneous index variation in the cross-sectional plane. As the dielectric / optical waveguides are of open-type structure, it is required to extend the problem domain to infinity. In extending the FEM to handle open-type waveguides, a particular scheme is needed to accommodate the infinite domain. In this connection, a variety of approaches have been proposed [1-3] introducing the use of infinite elements or the analytical solution for the exterior domain.

For the analysis of open waveguides, Yeh [3] uses the FEM with parametric infinite elements which incorporates a radial decay function of the form $\gamma = \exp(-\alpha r)$ where $\alpha > 0$. The asymptotic field behavior is therefore specified by the decay length $1/\alpha$, which is globally defined for the whole problem. One drawback of the formulation is that as at the outset the correct decay is unknown, an outer iteration loop is added to the FEM in which α parameter for each mode of interest is optimized.

The present formulation incorporates the unbounded region by employing infinite elements, which are combined with the standard finite elements. Since within the exterior unbounded domain, the general solutions to the field components are used as the interpolation function for the so called hybrid infinite elements, it eliminates the need for the outer iteration loop, which is imperative in Yeh's formulation. Adaptation of the two-node infinite elements to the finite

---

* Department of Electrical and Electronic Engineering

elements for the bounded domain doesn't increase the order or the bandwidth of the system matrix. Kishi [4] also makes use of the general solution for selecting the interpolation function for the infinite domain, but in that case, the system matrix turns into a full matrix. The present method provides a smooth combination of the infinite domain by utilizing formulations based on the hybrid variational principle. The governing and the discretized equations are presented in the following sections. Application of the formulation is made to some examples where the computed solutions are compared with the ones obtained by other methods.

2. VARIATIONAL FORMULATION

The cross-sectional geometry of a dielectric waveguide structure under consideration is shown in Fig.1, where the core is shown to be surrounded by the clad region which extends to infinity. The material properties of separate cross-sectional regions are assumed to be uniform along the direction of propagation. Consequently, the waveguiding problem could be defined by the two-dimensional eigenvalue formulation for the cross-section, where the variational formulation is derived by employing the longitudinal components of E and H. The governing equation for the longitudinal fields (assuming that E_z and H_z are not zero at the same time) of a guided wave propagating along the z direction can be represented [2] by the Helmholtz equation as

$$L \nabla^2 \phi + k_0^2 N \phi = 0 \qquad (1)$$

where $\phi = \{ \phi^H, \phi^E \} = \{H_z, (\omega \varepsilon_0 /\beta) E_z \}, L = \tau N$, with $\tau = (1-\varepsilon_{eff})/(\varepsilon_r - \varepsilon_{eff})$ and

$$N = \begin{bmatrix} 1 & 0 \\ 0 & \varepsilon_{eff} \varepsilon_r \end{bmatrix}, \text{ where } \varepsilon_{eff} = (\beta c_p/\omega)^2 : \text{effective dielectric, } \varepsilon_r : \text{relative permittivity}$$

$k_0^2 = (\omega/c_p)^2 (1-\varepsilon_{eff})$: wave number, ω : angular frequency, c_p : speed of light and β : propagation constant.

The electromagnetic fields are assumed to be propagating along the z direction with $\exp\{j (\omega t - \beta z)\}$. On the interface-boundary D between the core and the clad regions, the components $(E_s$ and H_s) of the fields tangential to the boundary, are to be continuous. The continuity conditions for the tangential field components are given by

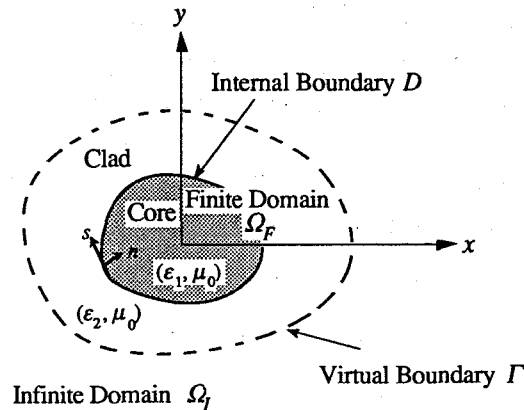$$E_{s_1} = E_{s_2}, \quad H_{s_1} = H_{s_2} \qquad (2)$$

Fig.1 Cross-section of an open-type dielectric waveguide

Here 1 and 2 represent the separate cross-sectional regions of different material properties. In the variational formulation, the longitudinal components of E and H are coupled at the interface boundaries.

As shown in Fig.1, the domain of the problem is divided into finite region Ω_F and infinite region Ω_I by imposing a

virtual boundary on the domain. At this instance, conventional finite elements are applied to the finite region Ω_F, while the infinite region Ω_I is represented by hybrid-type infinite elements.

2.1 Finite Region Formulation

The variational formulation corresponding to the propagation problem defined by Eq.(1) is given by

$$I_F(\phi) = \frac{1}{2}\iint_{\Omega_F} \nabla\phi^T L\nabla\phi \, dxdy - \frac{1}{2}k_0^2\iint_{\Omega_F} \phi^T N\phi \, dxdy - \int_D \phi^T \overline{M}\frac{\partial\phi}{\partial S}dl - j\int_\Gamma \phi^T K\psi \, dl \tag{3}$$

where $\psi = \{\psi^H, \psi^E\} = \{H_s, (\omega\varepsilon_0/\beta)E_s\}$, $\overline{M} = \tau\varepsilon_{eff}P$, $K = (\varepsilon_{eff}k_0^2/\beta)P$ where $P = \begin{bmatrix} 0 & 1 \\ -1 & 0 \end{bmatrix} = -P^T$

The discretized finite element formulation is obtained by assuming linear triangular elements so that after applying variational principle, the element formulation for the nodal unknowns of magnetic field ϕ_e^H and electric field ϕ_e^E is given by

$$\begin{bmatrix} \tau S_e & \tau\varepsilon_{eff}C_e \\ \tau\varepsilon_{eff}C_e^T & \tau\varepsilon_{eff}\varepsilon_r S_e \end{bmatrix}\begin{Bmatrix} \phi_e^H \\ \phi_e^E \end{Bmatrix} - k_0^2\begin{bmatrix} M_e & 0 \\ 0 & \varepsilon_{eff}\varepsilon_r M_e \end{bmatrix}\begin{Bmatrix} \phi_e^H \\ \phi_e^E \end{Bmatrix} = \begin{Bmatrix} Q_e^E \\ -Q_e^H \end{Bmatrix} \tag{4}$$

where $S_e = \iint_e \nabla\zeta_i \nabla\zeta_j \, dxdy$, $M_e = \iint_e \zeta_i\zeta_j \, dxdy$, $C_e = \int_{D_e} \zeta_i\frac{\partial\zeta_j}{\partial S}dl$

and $Q_e = j(\varepsilon_e k_0^2/\beta)\int_{\Gamma_e} \zeta_i\psi \, dl$ with $Q_e^a = j(\varepsilon_e k_0^2/\beta)\int_{\Gamma_e} \zeta_i\psi^a dl$, $(a = E, H)$

Here S_e, M_e, and C_e are the stiffness, mass and coupling matrices respectively, Q_e is the boundary driving term and $\zeta_{i,j}$ are the area coordinates. The element formulation given by Eq.(4) can be assembled for the entire domain to yield the global discretized formulation as

$$F\phi = Q \tag{5}$$

where $F = \begin{bmatrix} \tau S - k_0^2 M & \tau\varepsilon_{eff}C \\ \tau\varepsilon_{eff}C^T & \varepsilon_{eff}\varepsilon_r(\tau S - k_0^2 M) \end{bmatrix}$, $Q = \begin{Bmatrix} Q^E \\ -Q^H \end{Bmatrix}$

Q is driving term only on the boundary $(Q = Q_\Gamma)$ so that Eq.(5) can be partitioned as

$$\begin{bmatrix} F_F & F_{F\Gamma} \\ F_{\Gamma F} & F_{\Gamma\Gamma} \end{bmatrix}\begin{Bmatrix} \phi_F \\ \phi_\Gamma \end{Bmatrix} = \begin{Bmatrix} 0 \\ Q_\Gamma \end{Bmatrix} \tag{5'}$$

Q_Γ equals zero when there is no driving source on the virtual boundary of the domain, in which case, the system of the matrix equation given by Eq.(5) represents a standard eigenvalue problem.

2.2 Infinite Region Formulation

The formulations associated with the hybrid-type infinite element is based on the hybrid variational principle [5]. The related hybrid functional $I_H(\phi)$ corresponding to Eq.(1) for the infinite region Ω_I is given by

$$I_H(\phi) = -\iint_{\Omega_I} \phi^T L\nabla^2\phi \, dxdy - \frac{1}{2}\iint_{\Omega_I} \nabla\phi^T L\nabla\phi \, dxdy - \frac{1}{2}k_0^2\iint_{\Omega_I} \phi^T N\phi \, dxdy - \int_\Gamma \tilde{\phi}^T L\tilde{q}dl + \int_\Gamma \tilde{\phi}^T Lqdl \tag{6}$$

In Eq.(6), ϕ and $q (= \partial\phi/\partial n)$ are the potential and the flux respectively within the domain Ω_I, $\tilde{q}$ is the flux directed

normal to the boundary Γ (n is normal unit vector directed outward from the region Ω_I to the region Ω_F), and $\tilde{\phi}$ is the

unknown potentials defined on the boundary. The continuity of the electric field component $\bar{E}_s$ and magnetic field

component $\bar{H}_s$, which are tangential to the virtual boundary between finite and infinite regions, are incorporated in the

formulation by employing the equation

$$L\frac{\partial\tilde{\phi}}{\partial n} = L\tilde{q} = \bar{M}\frac{\partial\tilde{\phi}}{\partial S} + jK\tilde{\psi} \quad , \quad \text{where} \quad \tilde{\psi} = \{\tilde{\psi}^H, \tilde{\psi}^F\} = \{\bar{H}_s, (\omega\varepsilon_0/\beta)\bar{E}_s\} \tag{7}$$

Therefore, executing partial differentiation on the functional and making use of Eq.(1) leads to the equation given by

$$I_H(\phi) = -\frac{1}{2}\int_\Gamma \phi^T L q dl + \int_\Gamma \tilde{\phi}^T L q dl - \int_\Gamma \tilde{\phi}^T \bar{M}\frac{\partial\tilde{\phi}}{\partial S} dl - j\int_\Gamma \tilde{\phi}^T K\tilde{\psi} dl \tag{8}$$

As can be seen from Eq.(8), the functional for the infinite domain Ω_I is expressed only by line integrals along the boundary

Γ. Dividing the virtual boundary into a number of boundary elements and employing linear interpolation function ζ

(whose components are given in details in section 2.2.2), for the boundary element Γ_e, the discretized expression for $\tilde{\phi}_e$,

defined on the boundary is given for the element as

$$\tilde{\phi}_e = \zeta^T \tilde{\phi}_{\Gamma_e} \tag{9}$$

where $\tilde{\phi}_{\Gamma_e}$ comprises the nodal potentials located at the terminals of the element Γ_e. For the infinite domain, the potential ϕ

is expressed by the general solution to the Helmholtz equation with the form of an expanded series as

$$\phi = b^T A \tag{10}$$

where the vectors b and A represent respectively the undetermined multiplier and the general solution to the Helmholtz

equation, which are given in detail in the later section. Accordingly, the flux q along the normal direction is given by

$$q = \frac{\partial\phi}{\partial n} = b^T A_n \tag{11}$$

where A_n is the normal derivative of A. Substituting Eqs.(9)-(11) in the functional leads to the expression

$$I_{H_e}(\phi) = -\frac{1}{2}b^T L H_{\Gamma_e} b + \tilde{\phi}_e^T L G_{\Gamma_e} b - \tilde{\phi}_e^T \bar{M} X_{\Gamma_e} \tilde{\phi}_e - \tilde{\phi}_e^T P \tilde{Q}_{\Gamma_e} \tag{12}$$

for element e, situated adjacent to the boundary. The matrix terms of Eq.(12) are defined as

$$G_{\Gamma_e} = \int_{\Gamma_e} A_n \zeta^T dl \quad , \quad H_{\Gamma_e} = \int_{\Gamma_e} \frac{1}{2}(AA_n^T + A_n A^T) dl \quad , \quad X_{\Gamma_e} = \int_{\Gamma_e} \zeta\frac{\partial\zeta}{\partial S} dl \quad , \quad \tilde{Q}_{\Gamma_e} = j(\varepsilon_{eff} k_0^2/\beta)\int_{\Gamma_e} \zeta\tilde{\psi} dl \tag{13}$$

At this stage, discretizing the formulation for the boundary element Γ_e of the finite region and thereby, making it stationary

for $\tilde{\phi}_e^H$ and $\tilde{\phi}_e^E$, we obtain

$$\begin{bmatrix} \tau Y_{\Gamma_e} & \tau\varepsilon_{eff} X_{\Gamma_e} \\ \tau\varepsilon_{eff} X_{\Gamma_e}^T & \tau\varepsilon_{eff}\varepsilon_r Y_{\Gamma_e} \end{bmatrix}\begin{Bmatrix} \tilde{\phi}_{\Gamma_e}^H \\ \tilde{\phi}_{\Gamma_e}^E \end{Bmatrix} = \begin{Bmatrix} \tilde{Q}_{\Gamma_e}^E \\ -\tilde{Q}_{\Gamma_e}^H \end{Bmatrix} \tag{14}$$

This is a set of simultaneous equations associated with the nodes on boundary Γ_e, on which the effect of the exterior

domain is expressed. In Eq.(14), the term

$$Y_{\Gamma_e} = G_{\Gamma_e}^T H_{\Gamma_e}^{-1} G_{\Gamma_e} \tag{15}$$

is a hybrid-type infinite element matrix which is the admittance of the infinite region seen from boundary Γ_e. By

assembling Eq.(14), the equations for the entire boundary Γ yields the global discretized infinite element formulation

given by $I_{\Gamma\Gamma}\tilde{\phi}_\Gamma = \tilde{Q}_\Gamma$ for the entire infinite domain. Combining the infinite discretized formulation with the finite one given by Eq.(5)' leads to the final discretized formulation for the entire domain of the problem incorporating both the finite and the infinite regions. The compatibility conditions $\phi_\Gamma = \tilde{\phi}_\Gamma$ and $Q_\Gamma = -\tilde{Q}_\Gamma$ yield

$$\begin{bmatrix} F_{IF} & F_{FT} \\ F_{TF} & F_{TT} + I_{TT} \end{bmatrix} \begin{Bmatrix} \phi_F \\ \phi_\Gamma \end{Bmatrix} = \begin{Bmatrix} 0 \\ 0 \end{Bmatrix} \tag{16}$$

In the above hybrid formulation, the realization of the infinite region is made feasible by terminating the boundary of the finite region with the admittance $I_{\Gamma\Gamma}$.

2.2.1 Two Node Infinite Element

The two-dimensional general solution [4] for ϕ^H and ϕ^E of the infinite region Ω_I is given in terms of polar coordinate as

$$\phi^H = b_0 K_0(\chi r) + \sum_{m=1}^N b_m K_m(\chi r)\sin(m\theta + \rho) \quad , \quad \phi^E = b_0 K_0(\chi r) + \sum_{m=1}^N b_m K_m(\chi r)\cos(m\theta + \rho) \tag{17}$$

b_m is a coefficient to be determined, K_m (χr) is the Bessel function of second kind, m order, r is the distance from the origin to the point of interest, ρ is the phase angle which depends on the condition of symmetry of the corresponding eigen mode, and $\chi = [\beta^2 - (\omega/c)^2]^{1/2}$.

Here we consider some particular modes for which the parameters are chosen in accordance with the condition of E_z as shown in the Table 1.

Table 1 Selection of Parameters

Condition of symmetry for E_z		Mode Type	Parameter	
x axis	y axis		m	ρ
Symm.	Unsymm	E_{11}^x	odd	0
Unsymm	Symm.	E_{11}^y	odd	$\pi/2$

2.2.2 E^x Mode

While considering E^x mode, as we are concerned about the lower modes, truncation is made for which we take only two terms in Eq.(17) so that

$$\phi^H = b_0 K_0(\chi r) + b_1 K_1(\chi r)\sin\theta \quad , \quad \phi^E = b_0 K_0(\chi r) + b_1 K_1(\chi r)\cos\theta \tag{18}$$

Accordingly, $A^H = \{K_0 \quad sK_1\}$, $A^E = \{K_0 \quad cK_1\}$, $b = \{b_0 \quad b_1\}$ where the abbreviations used are given by

$$c = \cos\theta = \frac{x}{\sqrt{x^2+y^2}}, s = \sin\theta = \frac{y}{\sqrt{x^2+y^2}} \quad , \quad K_i = K_i(\chi r), K_i(j) = K_i(\chi r_j)$$

As shown in Fig.2, instead of considering the infinite region as a single element, it is divided radially to create infinite elements, which have two nodes on the boundary for each element. The other two nodes are supposed to be at infinity, where $\phi \rightarrow 0$ as $r \rightarrow \infty$. The infinite element matrix $Y_{\Gamma e}$ (Eq.(15)) is now evaluated or integrated for the boundary (1-2-3-4) surrounding the region shown in Fig.2. The integration scheme for the edge-components of $G_{\Gamma e}$ and $H_{\Gamma e}$ is carried out

as

$$G_{\Gamma_e} = G_{12} + G_{23} + G_{41} \quad \text{and} \quad H_{\Gamma_e} = H_{12} + H_{23} + H_{41} \tag{19}$$
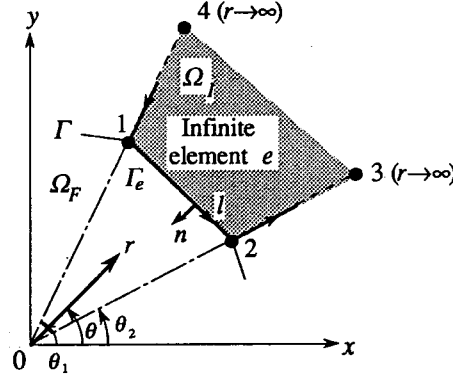

Fig.2 Two node infinite element

At first, the finite boundary 1-2 is considered where the general solution of the vector A and its normal derivative A_n take the following form

$$A_n = \{ A_{n_0} \ A_{n_1} \} \ , \quad A_{n_0}^H = A_{n_0}^E = -\chi(cn_x + sn_y)K_1 \ ,$$

$$A_{n_1}^H = \chi s(cn_x + sn_y)\left(-K_0 - \frac{K_1}{\chi r}\right) + c\left(\frac{-s}{r}n_x + \frac{c}{r}n_y\right)K_1 \ ,$$

$$A_{n_1}^E = \chi c(cn_x + sn_y)\left(-K_0 - \frac{K_1}{\chi r}\right) + s\left(\frac{s}{r}n_x - \frac{c}{r}n_y\right)K_1 \tag{20}$$

Here $n_x = (y_2 - y_1) / l_{12}$, $n_y = (x_1 - x_2) / l_{12}$, where l_{12} is the length of the boundary element Γ_e, and n_x and n_y are the cosine angles made respectively with the x and y axes. Accordingly, G_{12} is given as

$$G_{12} = \frac{1}{2} l_{12} \int_{-1}^{1} \begin{bmatrix} A_{n_0}\zeta_1 & A_{n_0}\zeta_2 \\ A_{n_1}\zeta_1 & A_{n_1}\zeta_2 \end{bmatrix} d\xi \tag{21}$$

Here $\zeta_1 = (1 - \xi) / 2$ and $\zeta_2 = (1 + \xi) / 2$ for the linear interpolation assumed where ξ is the local coordinate $(-1 \le \xi \le 1)$. Again H_{12} is given as

$$H_{12} = \frac{1}{2} l_{12} \int_{-1}^{1} \begin{bmatrix} A_0 A_{n_0} & \frac{1}{2}(A_0 A_{n_1} + A_1 A_{n_0}) \\ \frac{1}{2}(A_0 A_{n_1} + A_1 A_{n_0}) & A_1 A_{n_1} \end{bmatrix} d\xi \tag{22}$$

Note that the integration in the above equations can easily be carried out by using Gaussian quadrature formula. However, since the integration along the infinite interelement boundary or edge 2-3 is directed radially along r, cylindrical coordinate system is introduced. Realizing $\partial / \partial n = (-1 / r) \partial / \partial \theta$, $\theta = \theta_2$ and $dl = dr$, we obtain

$$A^H = \{K_0 \ \ s_2 K_1\}, A^E = \{K_0 \ \ c_2 K_1\} \ , \quad A_n^H = \left\{0 \ \ \frac{-1}{r} c_2 K_1\right\}, A_n^E = \left\{0 \ \ \frac{1}{r} s_2 K_1\right\} \tag{23}$$

where $c_i = \cos \theta_i$, $s_i = \sin \theta_i$, $\zeta_{23} = \{ 0 \quad K_0 / K_0(2) \}$. Again for the edge 4-1, $\zeta_{41} = \{ K_0 / K_0(1) \quad 0 \}$, $\partial / \partial n = (1 / r) \partial / \partial \theta$, $\theta = \theta_1$ and $dl = dr$ so that the expressions for A and A_n are obtained by just replacing the subscript of the expressions for the edge 2-3 and putting $\theta_1 = \theta_2$ yielding

$$A^H = \{K_0 \ \ s_1 K_1\}, A^E = \{K_0 \ \ c_1 K_1\} \ , \quad A_n^H = \left\{0 \ \ \frac{1}{r} c_1 K_1\right\}, A_n^E = \left\{0 \ \ \frac{-1}{r} s_1 K_1\right\} \tag{24}$$

And accordingly, the part of the matrices G and H that correspond to the infinite edges (interelement boundaries) 2-3 and 4-1 are given by

$$G_{23}^{H} + G_{41}^{H} = \begin{bmatrix} 0 & 0 \\ \dfrac{c_1}{K_0(1)} J_{011} & \dfrac{-c_2}{K_0(2)} J_{012} \end{bmatrix} \ , \quad G_{23}^{E} + G_{41}^{E} = \begin{bmatrix} 0 & 0 \\ \dfrac{-s_1}{K_0(1)} J_{011} & \dfrac{s_2}{K_0(2)} J_{012} \end{bmatrix}$$

$$H_{23}^{H} + H_{41}^{H} = \begin{bmatrix} 0 & \dfrac{-c_2}{2} J_{012} + \dfrac{c_1}{2} J_{011} \\ \dfrac{-c_2}{2} J_{012} + \dfrac{c_1}{2} J_{011} & -s_2 c_2 J_{112} + s_1 c_1 J_{111} \end{bmatrix} \ , \quad H_{23}^{E} + H_{41}^{E} = \begin{bmatrix} 0 & \dfrac{s_2}{2} J_{012} - \dfrac{s_1}{2} J_{011} \\ \dfrac{s_2}{2} J_{012} - \dfrac{s_1}{2} J_{011} & s_2 c_2 J_{112} - s_1 c_1 J_{111} \end{bmatrix}$$

$$(25)$$

Where $J_{ijk} = \displaystyle\int_{r_i}^{\infty} K_i K_j \frac{dr}{r}$, $\displaystyle\int_{r_i}^{\infty} K_0 K_1 \frac{dr}{r} = \chi r_i \left\{ K_0^2(i) + \frac{K_0(i)K_1(i)}{\chi r_i} - K_1^2(i) \right\}$

so that J_{111} and J_{112} are the only terms for which numerical integrations are needed to be carried out. G_{r_e} and H_{r_e} are evaluated from Eq.(19) and Y_{r_e} is evaluated from Eq.(15). Note that the corresponding two node infinite element matrix attains the order of 2×2 for node 1 and 2.

2.2.3 E^y Mode

As shown for the E^x mode, for $N = 1$ and $\rho = \pi / 2$, the following expressions are obtained for the E^y mode.

$$\phi^H = b_0 K_0(\chi r) + b_1 K_1(\chi r)\sin(\theta + \pi/2) = b_0 K_0(\chi r) + b_1 K_1(\chi r)\cos\theta$$
$$\phi^E = b_0 K_0(\chi r) + b_1 K_1(\chi r)\cos(\theta + \pi/2) = b_0 K_0(\chi r) - b_1 K_1(\chi r)\sin\theta$$

$$(26)$$

Regarding the finite edge 1-2, the expressions for vector A and its normal derivative A_n are given by

$$A_{n_0}^{H} = A_{n_0}^{E} = -\chi(cn_x + sn_y)K_1 \ , \quad A_{n_1}^{H} = \chi c(cn_x + sn_y)\left(-K_0 - \frac{K_1}{\chi r}\right) + s\left(\frac{s}{r} n_x - \frac{c}{r} n_y\right)K_1$$

and $\quad A_{n_1}^{E} = -\chi s(cn_x + sn_y)\left(-K_0 - \frac{K_1}{\chi r}\right) + c\left(\frac{s}{r} n_x - \frac{c}{r} n_y\right)K_1$

$$(27)$$

G_{12} and H_{12} are evaluated using the Eqs.(21) and (22) respectively, and the part of the matrices G and H that correspond to the infinite edges 2-3 and 4-1 are given by

$$G_{23}^{H} + G_{41}^{H} = \begin{bmatrix} 0 & 0 \\ \dfrac{-s_1}{K_0(1)} J_{011} & \dfrac{s_2}{K_0(2)} J_{012} \end{bmatrix} \quad G_{23}^{E} + G_{41}^{E} = \begin{bmatrix} 0 & 0 \\ \dfrac{-c_1}{K_0(1)} J_{011} & \dfrac{c_2}{K_0(2)} J_{012} \end{bmatrix}$$

$$(28)$$

$$H_{23}^{H} + H_{41}^{H} = \begin{bmatrix} 0 & \dfrac{s_2}{2} J_{012} - \dfrac{s_1}{2} J_{011} \\ \dfrac{s_2}{2} J_{012} - \dfrac{s_1}{2} J_{011} & s_2 c_2 J_{112} - s_1 c_1 J_{111} \end{bmatrix} \quad H_{23}^{E} + H_{41}^{E} = \begin{bmatrix} 0 & \dfrac{c_2}{2} J_{012} - \dfrac{c_1}{2} J_{011} \\ \dfrac{c_2}{2} J_{012} - \dfrac{c_1}{2} J_{011} & -s_2 c_2 J_{112} + s_1 c_1 J_{111} \end{bmatrix}$$

3. NUMERICAL EXAMPLES

In order to demonstrate the application and quality of the method presented in the previous section, the solutions for a couple of sample problems are given and are compared with the solutions obtained by different methods. The first example taken is that of a circular step-index fiber (shown in Fig.3), for which the modal solution is obtained. The

boundary conditions and the element divisions are shown in Fig.4. For symmetry, only one quarter of the structure is taken for the analysis. The infinite elements are applied at the boundary R_0. The dispersion curve for the propagating mode

HE_{11}^y with $n_1 = \sqrt{\varepsilon_1} =1.0$, $n_2 = \sqrt{\varepsilon_2} =1.01$ and $R_0 / a = 5.0$ is shown in Fig.5.
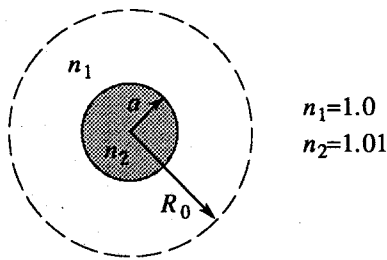

$n_1=1.0$
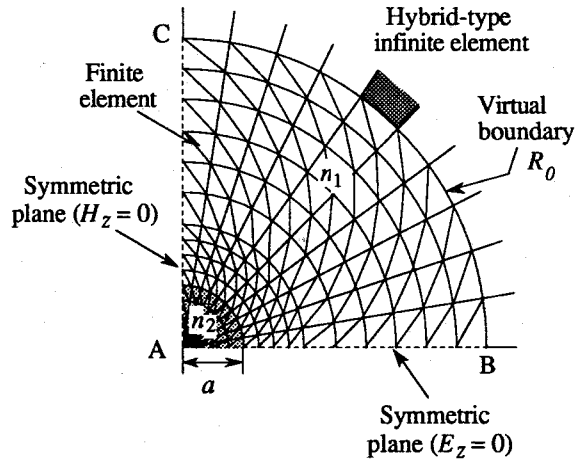$n_2=1.01$

Fig. 3   Step-index fiber

Fig. 4   Finite element model

Note that HE_{11}^y is a hybrid mode where $H_z > E_z$ and the superscript y indicates the direction along which the electric field is dominant. In Fig.5, + symbol represents the solutions obtained by the present hybrid formulation employing both finite and infinite elements, o represents the one obtained by employing only the finite elements having the domain bounded by imposing the boundary condition $E_z = 0$ at the virtual boundary and Δ represent the spurious solutions encountered by the
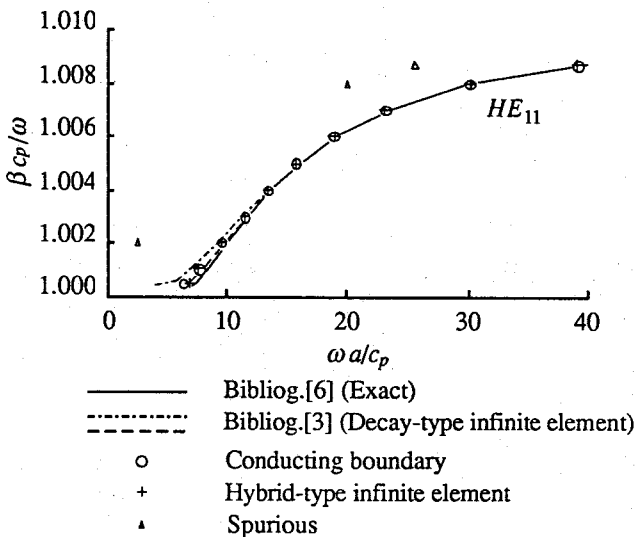

HE_{11}

──────── Bibliog.[6] (Exact)
── ── ── Bibliog.[3] (Decay-type infinite element)
    o   Conducting boundary
    +   Hybrid-type infinite element
    ▲   Spurious

Fig. 5   Dispersion curve for the step-index fiber

A   Magnetic field   Electric field   B

──────── Hybrid-type infinite element

------------ Conducting boundary
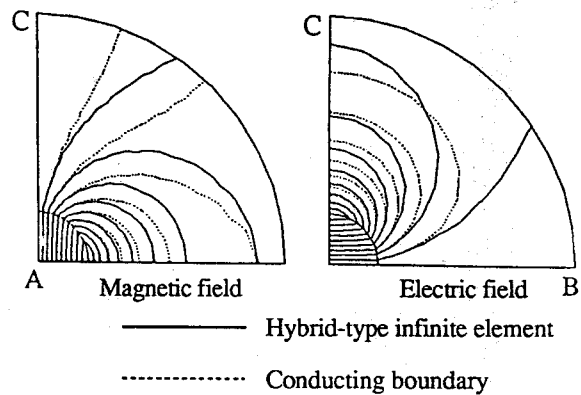
Fig. 6   Field distribution at $\beta c_p/\omega$=1.0005
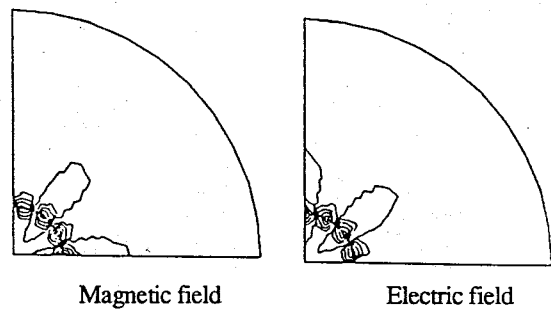

Magnetic field   Electric field

Fig. 7   Spurious modes at $\beta c_p/\omega$ =1.002

present method. The solutions obtained by the present method are compared with the exact ones [6] and the ones obtained by Yeh [3]. The accuracy of the present method has been found satisfactory. However, from the figure, it looks that the outer boundary condition doesn't have much effect on the dispersion curve.

In Ref.[3], Yeh uses decay-type infinite elements and employs 157 and 588 quadrilateral elements for a R_0 / a of 14 and 42 respectively. It is quite evident that to achieve good accuracy at low frequency solution by Yeh's method, large finite domain (a large value of R_0 / a as well as a large number of elements) is required. Regarding the present formulation, due to the presence of the frequency term in the infinite element matrix, inclusion of the effect of the infinite domain destroys the standard eigenvalue matrix expression. To obtain eigenvalues, the determinant search technique must be used. What make the present method very efficient are that inclusion of the infinite elements doesn't increase the bandwidth, and that small number of elements are required for reasonable accuracy.

In Fig.6, the magnetic and the electric field distributions for an effective dielectric of $\beta c_p/\omega = 1.0005$ are shown. In the figure, the dotted lines represent the field distributions for the bounded case obtained by employing only the finite elements and the solid lines represent the one for the unbounded case obtained by employing both the finite and the infinite elements. It is quite clear from the figure that for the bounded case, the fields confine inside the assumed boundary while for the unbounded case, the fields spread out towards the infinite region. The difference will be more pronounced for the core with lower refractive index. In the present analysis, we encounter the spurious modes. The field distributions for a spurious mode is shown in Fig.7, which could be noticed and removed without difficulty. There are reports [2, 7] regarding the places of occurrence, origin and elimination of the spurious modes.

$$a = b = 4.0mm$$
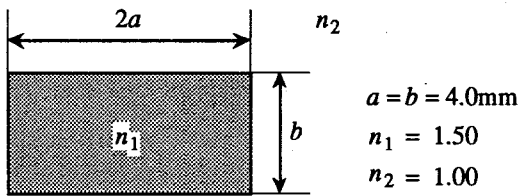$$n_1 = 1.50$$
$$n_2 = 1.00$$

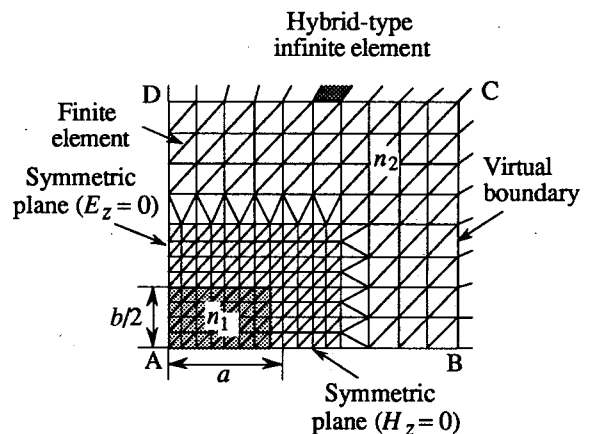Fig. 8   Rectangular dielectric waveguide

Fig. 9   Finite-element model

Next, employing the present method, simulation is carried out for the rectangular dielectric waveguide of Fig.8. The boundary conditions and the element divisions are shown in Fig.9. The dispersion curve, shown in Fig.10 is obtained

———— Bibliog.[8] (Circular harmonic expansion tech.)
– – – – – Bibliog.[9] (Marcatili's method)

$$B = (\omega / c_p) b \sqrt{n_2^2 - n_1^2} / \pi \qquad : \text{Normalized frequency}$$

$$P^2 = [(\beta c_p/\omega)^2 - n_1^2] / (n_2^2 - n_1^2) \qquad : \text{Normalized propagation constant}$$
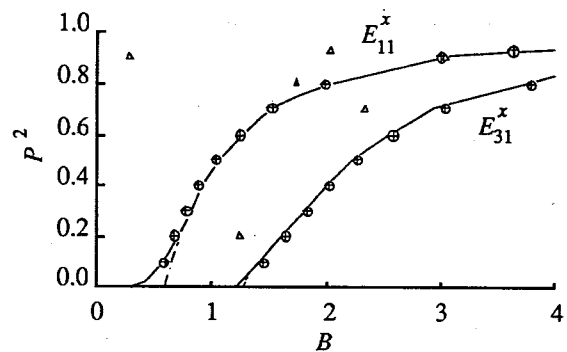

Fig. 10   Dispersion curve for the rectangular dielectric waveguide

for the propagating mode E^x (where E_x and H_y are the major field components) taking one quarter of the symmetric structure for the simulation with $n_1 = 1.0$, $n_2 = 1.5$ and $a/b = 1$. For comparison, solutions obtained by other methods [8, 9] are also shown which are found to be in well agreement with the ones obtained by the present method. Though dispersion characteristic with similar accuracy can be obtained by the finite element solutions assuming the guide to be bounded by the conducting boundary, as in the previous case, the electric field distributions obtained from the bounded solutions are less practical than the one obtained by the unbounded solutions employing both finite and infinite elements. In Fig.11, the electromagnetic field distributions are shown for the modes E_{11}^x and E_{31}^x.

E_{11}^x mode E_{31}^x mode

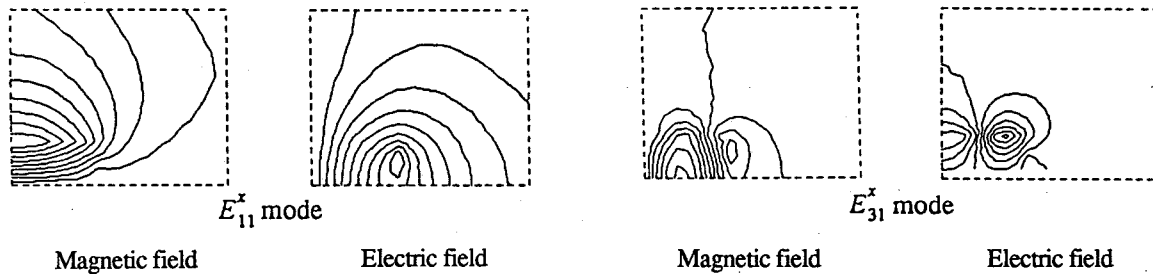Magnetic field   Electric field   Magnetic field   Electric field

Fig. 11   Field Distribution at $P^2 = 0.1$

4. CONCLUSIONS

A finite element method for the propagation analysis of unbounded, arbitrarily shaped, dielectric / optical waveguide structures has been proposed where the unbounded region is accommodated through the use of hybrid infinite elements. Numerical analysis is carried out for a circular step-index fiber and a rectangular dielectric / optical waveguide, where the incorporation of the unbounded region is shown feasible for symmetric waveguide structures. The merit of the present method is, extension of the finite element formulation to accommodate the infinite elements doesn't cause any change in the order of the system matrix and also in the bandwidth. The solution procedure is therefore very efficient despite the fact that the hybrid formulation can't be solved by the standard eigenvalue solver as the wave number spreads out in the formulation in a scattered manner, and determinant search technique must be used. What offsets the merits is the occurrence of spurious modes along with the physical ones. But again, the spurious modes could be detected easily and removed thereby.

REFERENCES

[1] Y.Kagawa : "Finite and Boundary Element Methods for Unbounded Field Problems", Science-sha, Tokyo (1983).

[2] Y.Kagawa, M.Koshiba, M.Ikeuchi and S.Kagami : "Finite and Boundary Element Methods for Electrical Engineers - Application to Wave Problems", Ohm-sha, Tokyo (1984).

[3] C.Yeh, K.Ha, S.B.Dong and W.P.Brown : "Single-mode optical waveguide", Appl.Opt., vol.18, pp.1490-1504, (1979).

[4] N.Kishi and T.Okoshi : "Boundary integral method without Green's function (part 2) - Application to the modal analysis of optical fibers", Research Meeting Record, The Institute of Electrical Engineers of Japan, EMT-78, pp.59-68,

(1985).

[5] P.Tong and J. N.Rossettos :" Finite-Element Method", MIT Press, London, (1982).

[6] J.Carson, S.P.Mead and S.A.Schelkunoff , Bell Syst. Tech. J., 15, pp.310, (1936).

[7] M.Ikeuchi, K.Inoue, H.Sawami and H.Niki : "Spurious solutions in the finite element analysis of micro-strip lines", The Transaction of The Institute of Electrical Engineers of Japan, vol.98-A, pp.415-422, (1978).

[8] J.E.Goel : "A circular harmonic computer analysis of rectangular dielectric waveguides", Bell Sys.Tech.J., vol.48, pp.2133-2160, (1969).

[9] E.A.J.Marcatili : "Dielectric rectangular waveguide and directional coupler for integrated optics", Bell Sys.Tech.J., vol.48, pp.2071-2102, (1969).